Heterogeneity of DMIPP Uptake and Its Relationship with Heterogeneous Myocardial Blood Flow

Gerrit W. Sloof, Frans C. Visser, Emile F.I. Comans, Albert B.J. Groeneveld, Jeroen J. Bax, Machiel J. van Eenige, Ger J. van der Vusse and Furn F. (Russ) Knapp, Jr.

Departments of Nuclear Medicine, Cardiology and Internal Medicine, Free University Hospital, Amsterdam, The Netherlands; Department of Physiology, Cardiovascular Research Institute, University of Limburg, Maastricht, The Netherlands; and Nuclear Medicine Group, Oak Ridge National Laboratory, Oak Ridge, Tennessee

To assess its potential role as a new metabolic probe, the relationship between regional uptake of the 15-(p-[^{125}I]-iodophenyl)-3,3-dimethylpentadecanoic acid (DMIPP) fatty acid analog and myocardial blood flow was studied. **Methods:** In 14 open-chest dogs, the left anterior descending coronary artery was cannulated and extracorporal bypass-perfused at normal (control group; n = 4) and reduced flow (intervention group; n = 10). Myocardial blood flow (MBF) was assessed with ^{46}Sc-labeled microspheres. Forty minutes after intravenous injection of DMIPP, the heart was excised and cut into 120 samples. In each sample, MBF ml · g^{-1} · min^{-1} and DMIPP uptake (percentage of the injected dose per gram, %ID/g) were assessed. **Results:** In normal myocardium, MBF and DMIPP uptake were 1.10 ± 0.18 ml · g^{-1} · min^{-1} and 1.18 ± 0.42 × 10^{-2} %ID/g, respectively. In the extracorporal bypass area, flow was reduced to 0.49 ± 0.20 ml · g^{-1} · min^{-1} ($p < 0.0001$ compared to normal), and DMIPP uptake was decreased to 0.75 ± 0.26 × 10^{-2} %ID/g ($p < 0.0001$ compared to normal). DMIPP uptake and MBF positively correlated in normal (DMIPP uptake = 0.77 ± 0.23 · MBF; $r = 0.41$; $p < 0.0001$) and hypoperfused (DMIPP uptake = 0.35 ± 0.70 · MBF; $r = 0.63$; $p < 0.0001$) myocardium. The heterogeneity, indicated by the coefficient of variation, in normal myocardium was 0.23 ± 0.05 for MBF and was lower ($p < 0.0001$) for DMIPP uptake: 0.13 ± 0.05. During flow reduction, heterogeneity increased significantly ($p < 0.0001$) for both MBF (0.59 ± 0.22) and DMIPP uptake (0.37 ± 0.23). Also heterogeneity of the DMIPP uptake to MBF ratio, as an indicator of agreement, increased from 0.23 ± 0.07 in normal to 0.46 ± 0.19 in hypoperfused myocardium ($p < 0.0001$). **Conclusion:** DMIPP detects regionally hypoperfused myocardium, in which agreement between MBF and fatty acid uptake deteriorates. DMIPP uptake shows a different relationship with MBF in hypoperfused compared to normal myocardium. These observations suggest that DMIPP uptake may provide additional, unique information on regional myocardial ischemia.

Key Words: iodinated fatty acids; myocardial blood flow; heterogeneity

J Nucl Med 1997; 38:1424–1430

Under physiological conditions, long-chain fatty acids are the main source for oxidative myocardial energy production (*1,2*). Despite the complexity of fatty acid homeostasis, scintigraphy with fatty acid analogs can provide information on discrete aspects of fatty acid metabolism that involve uptake, oxidation or lipid incorporation. A variety of radioiodinated fatty acids (IFAs) have been developed to study cardiac fatty acid metabolism noninvasively in man (*3,4*). In recent years, myocardial fatty acid imaging has focused on IFAs showing prolonged myocardial retention, thus permitting regional myocardial distribution studies by SPECT (*5,6*). Introduction of methyl-branching of the aliphatic chain of the fatty acid molecule appeared to be a successful approach to delay myocardial clearance by inhibiting myocardial oxidation. The monomethyl-branched analog 15-(p-iodophenyl)-3-R,S-methylpentadecanoic acid (BMIPP) has been most intensively studied in animal models and evaluated in patients (*5,6*), and it has been demonstrated that BMIPP uptake patterns correspond well with [^{11}C]palmitate uptake in patients with coronary artery disease (*7*). However, BMIPP showed some myocardial clearance due to catabolism by initial alpha-oxidation followed by cycles of beta-oxidation (*5,8–12*). Therefore, Knapp et al. (*9*) developed 15-(p-iodophenyl)-3,3-dimethylpentadecanoic acid (DMIPP), in which beta-dimethyl-substitution leads to more effective inhibition of catabolism. In dogs, DMIPP showed considerable myocardial uptake and prolonged retention, reflected by predominant incorporation into triacylglycerols and high heart to blood ratios: 12.7 ± 3.7:1 (*13*). These properties make DMIPP a promising tracer for studying regional fatty acid uptake by SPECT (*13*). Nevertheless, the uptake kinetics of DMIPP in hypoperfused relative to normal myocardium requires detailed evaluation.

Myocardial blood flow (MBF) is heterogeneous, both transmurally and circumferentially (*14–25*). The observed heterogeneity is greater than can be accounted for by error due to the technique of blood flow measurements (*16,19,21*) and larger than temporal variability (*14–16*). Causes for this spatial heterogeneity have not yet been elucidated. Differences in regional metabolism have been suggested (*18,23–25*), although conflicting results have been observed (*26*). During ischemia, heterogeneity in MBF becomes highly pronounced (*21,27*). Because of factors such as severity and duration of flow reduction, this heterogeneity may play an important role in heterogeneous myocardial damage (focal necrosis).

Knowledge of heterogeneity of myocardial fatty acid uptake is virtually lacking; however, this might be crucial for the comprehension of scintigraphic data obtained in patients. The aim of this study was, therefore, to assess the heterogeneity of DMIPP uptake in relation to the heterogeneous blood flow, both in normal and hypoperfused myocardium.

MATERIALS AND METHODS

Fourteen male mongrel dogs (27.5 ± 2.9) were studied after overnight fasting. After premedication with 2.0–4.0 ml of Thalamonal intramuscularly (2.5 mg of droperidol/50 μg of fentanyl per ml), anesthesia was induced by fentanyl (20 μg/kg) through a cannula in a cephalic vein, immediately followed by administration of etomidate (0.4 mg/kg). Before thoracotomy, droperidol (0.5

Received Oct. 11, 1996; accepted Nov. 23, 1996.

For correspondence or reprints contact: Gerrit W. Sloof, MD, Department of Nuclear Medicine, Free University Hospital, De Boelelaan 1117, 1081 HV Amsterdam, The Netherlands.

mg/kg) and fentanyl (40 μg/kg) were administered by bolus injection, followed by continuous infusion of fentanyl (10–20 $\mu g \cdot kg^{-1} \cdot hr^{-1}$). The dogs were ventilated with $N_2O:O_2$ (2:1, v/v), and muscle relaxation was maintained with pancuronium intravenously (0.2 mg/kg prior intubation, followed by 0.01 $mg \cdot kg^{-1} \cdot hr^{-1}$). Arterial blood gas samples were taken every 30 min, and ventilation was adjusted in such a way that proper blood gas levels were maintained, i.e., PO_2 of about 13.3 kPa and PC_{O_2} of about 5.0 kPa. The pH was maintained at 7.4 by administering sodium hydrogen carbonate ($NaHCO_3$, 4.2%) when required.

A catheter was introduced into the carotid artery for blood sampling and arterial pressure measurements. For measurements of cardiac output and central body temperature, a pulmonary artery catheter was introduced into the external jugular vein. A thoracotomy was performed through the fifth left intercostal space, and the heart was suspended in a pericardial cradle. To prevent blood clotting, heparin 200 units/kg intravenously was given. The electrocardiogram and pressure curves were continuously monitored, and central body temperature was maintained between 37°C and 38°C using a water-heated pad. Normal saline was infused to match losses due to respiration and blood sampling.

Experimental Protocols

After thoracotomy, the proximal left anterior descending coronary artery (LAD) was isolated and cannulated with an 18-gauge polyethylene cannula. Immediately (several seconds) after cannulation, the LAD area was perfused with arterial blood withdrawn from a catheter in a femoral artery by an extracorporal bypass (ECB) system; the volume of the system was 18 ml. The LAD proximal to the site of cannulation was ligated, and a calibrated roller pump was used to adjust coronary flow. The perfusion pressure was measured at the proximal entrance of the cannula. The temperature of the blood was maintained at central body temperature by means of a heat exchanger (countercurrent principle). To obtain normal flow, the perfusion pressure was adjusted to match mean aortic pressure.

Two groups of animals were investigated: in a control group (n = 4), the LAD flow was maintained on a normal level to assess any effects of the ECB procedure on MBF and DMIPP uptake. In an intervention group (n = 10), the LAD flow was reduced to one-third by the ECB.

Twenty-five minutes after adjusting (t = 0 min) the LAD flow in both groups, MBF was measured by the radiolabeled microsphere technique (*28*). Scandium-46-labeled microspheres (ϕ = 15 ± 1 μm; half-life = 83.8 days; gamma-peak energy = 889 and 1121 keV; specific activity = 8×10^3 spheres/kBq) were suspended in normal saline and one drop of Tween 80 and thoroughly mixed using a vortex shaker. Mixing was continued until injection through a cannula in the left atrium, and approximately 3 million microspheres (370 kBq) were injected. Withdrawal of the arterial reference sample at the site of a carotid artery was initiated just before the injection of microspheres and was continued for 2 min at a rate of 18.2 ml/min using a roller pump. At t = 30 min, 34 ± 4 MBq DMIPP (half-life = 60.2 days; gamma-peak energy = 35 keV; specific activity = 296 MBq/mg) was injected into the cephalic vein. At t = 70 min, black Indian ink was administered into the ECB system to determine the ECB-perfused region, immediately followed by intracavitary administration of potassium chloride to induce cardiac arrest.

After cardiac arrest, the heart was rapidly excised and rinsed in ice-cold saline. After removal of the atria, right ventricle, valves and subepicardial fat, the left ventricle (LV) (weight = 123.5 ± 20.7 g) was cut into five equal-thickness, transverse slices parallel to the atrioventricular A-V ring. The slices were cut into eight radial segments, each divided into subepi-, mid- and subendocardial samples. The samples were classified as being entirely stained, i.e., ECB region in control and intervention hearts, or not stained at all, i.e., native perfused myocardium. Partially stained samples were classified as borderline. After weighing the myocardial samples (mean ± s.d., 1.080 ± 0.394 g) and blood reference samples, the radioactivity was counted for 5 min in a gamma well counter, with settings appropriate for ^{125}I (window, 20–81 keV, which includes the coincidence peak in the well counter) and ^{46}Sc (window, 756–1268 keV). Correction was made for background, decay and cross-over. Cross-over was 7.7% for ^{46}Sc into the ^{125}I and negligible for the opposite situation. Because countrates for ^{125}I were manyfold of those of ^{46}Sc, the cross-over caused no serious problem for counting statistics (see Appendix). From the weights and activity, the MBF ($ml \cdot g^{-1} \cdot min^{-1}$) and DMIPP uptake (%ID/g) values were calculated for the samples.

Data Analysis

Data from the experiments are presented as absolute values. To reduce variation between dogs and to allow graphic presentation, the data were pooled after normalization of the individual samples to the mean value of the normal myocardium in each individual dog.

Distributions of MBF, DMIPP uptake and the ratios in the native and ECB-perfused myocardium appeared Gaussian ($p > 0.05$, one-sample Kolomogorov-Smirnov test) in each individual dog as well as in pooled data. Heterogeneity was expressed as the coefficient of variation (s.d. mean), and to test statistical significance, the t-test for paired or unpaired data was used.

To study the relationship between MBF and DMIPP uptake, linear regression analysis was applied and significance was tested with one-way ANOVA. Multiple regression analysis with dummy variables to denote hypoperfused or normal myocardium was used to compare regression lines, and significance was tested with the F-test. The correlation coefficient, as a result of linear regression analysis, is determined by, among other factors, the slope, range of values and agreement of the variables. To have a more objective parameter for the degree of agreement between DMIPP uptake and MBF, their ratios in the individual samples were calculated. The agreement between MBF and DMIPP uptake was expressed by the coefficient of variation of the ratios; a high value indicates a low agreement. All statistical differences were considered significant if the probability was less than 0.05.

RESULTS

Hemodynamics and Substrate Levels

Hemodynamic parameters and arterial substrate levels are summarized in Table 1. In controls, mean arterial pressure, heart rate and cardiac output were stable during the entire procedure. In the intervention group, heart rate increased over time, and mean arterial pressure was stable until the moment of DMIPP administration but decreased at the end of the experiment. The cardiac output decreased slightly yet remained within normal limits. Arterial levels of glucose, lactate and B-hydroxybutyrate were in normal ranges and did not change significantly during the experiment. Concentrations of (unlabeled) fatty acids were in the upper normal range.

Control Group

Values of MBF, DMIPP uptake and subendo-to-subepicardial ratios for both MBF and DMIPP uptake in the ECB-perfused myocardium (115 samples) were not significantly different from values for the native perfused myocardium (365 samples) in controls (n = 4) (Table 2). Neither heterogeneity nor agreement of MBF and DMIPP uptake were significantly different between native and ECB-perfused myocardium. Thus, within normal flow values, application of the ECB technique

TABLE 1
Hemodynamic Variables and Plasma Levels of Substrates in the Control and Intervention Group

	Time (min)	Control (n = 4)	Intervention (n = 10)
Hemodynamics			
Mean arterial pressure	0	110 ± 15	108 ± 13
(mmHg)	30	112 ± 14	103 ± 11
	70	107 ± 10	86 ± 20*
Heart rate (beats/min)	0	125 ± 25	121 ± 26
	30	122 ± 21	145 ± 31*
	70	122 ± 8	156 ± 28*
Cardiac output (liters/min)	0	4.6 ± 1.1	5.0 ± 1.1
	30	4.4 ± 0.2	4.7 ± 0.5
	70	4.3 ± 0.3	4.2 ± 0.9*
Substrates (mmol/liter)			
Fatty acids		0.78 ± 0.50	0.88 ± 0.33
Glucose		7.8 ± 0.5	8.0 ± 1.7
Lactate		2.7 ± 2.2	2.2 ± 1.8
B-hydroxybutyrate		0.06 ± 0.04	0.05 ± 0.03

*$p < 0.05$ vs. t = 0.
Data are expressed as mean ± s.d. Arterial substrate levels at time of DMIPP administration (t = 30 min).

did not alter the characteristics of blood flow and DMIPP uptake.

The distribution of MBF and DMIPP uptake in the pooled samples (n = 480) of the four normal LVs, expressed as the percentage of the LV mass, both show a normal, Gaussian distribution (Fig. 1). Heterogeneity of MBF and DMIPP uptake was significantly different: 0.23 ± 0.06 and 0.13 ± 0.05, respectively ($p < 0.0001$; Table 2). The difference in heterogeneity is also indicated by the width of the curve of the distribution profile (Fig. 1); for pooled data, heterogeneity was 0.23 for MBF and 0.15 for DMIPP uptake.

Intervention Group

The number of samples in the intervention area of the 10 dog hearts ranged from 15 to 30, representing 10.4%–25.2% of the LV mass. There was a significant flow reduction in the ECB area of each of the 10 dog hearts ($p < 0.0001$ for each individual experiment).

In native perfused, normal myocardium MBF and DMIPP uptake were 1.10 ± 0.18 ml · g^{-1} · min^{-1} and 1.18 ± 0.42 × 10^{-2} %ID/g, respectively. In the ECB area, flow was significantly reduced to 0.49 ± 0.20 ml · g^{-1} · min^{-1} ($p < 0.0001$ compared to normal), in which DMIPP uptake was significantly decreased to 0.75 ± 0.26 × 10^{-2} %ID/g ($p < 0.0001$ compared to normal). Subendo-to-subepicardial ratios for both MBF and DMIPP uptake decreased significantly in hypoperfused versus normal myocardium (Table 2).

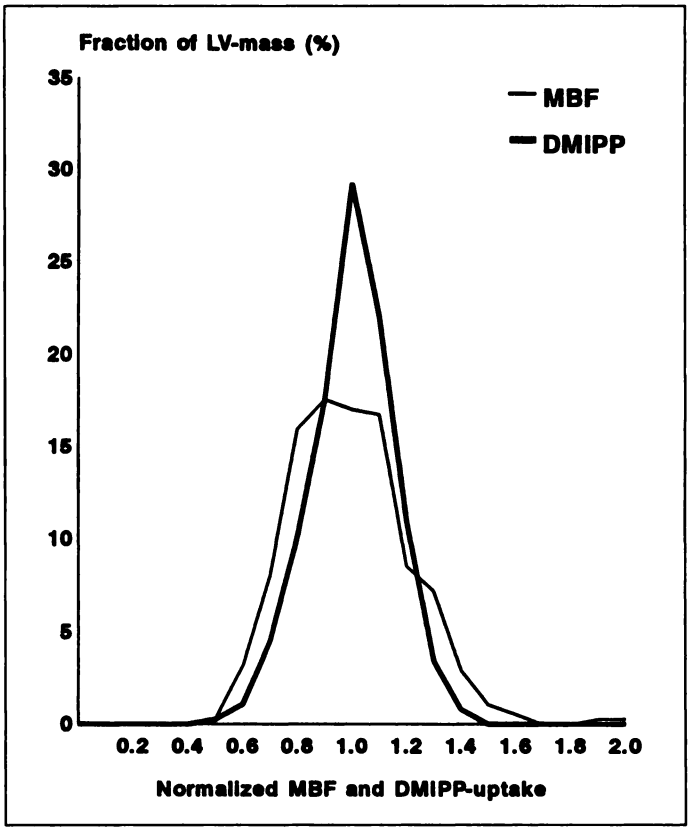

FIGURE 1. Frequency histogram (percentage of LV mass) of MBF and DMIPP uptake, normalized for respective mean values in each dog (480 samples of four normoxic left ventricles; control experiments).

Linear regression analysis for pooled data (Fig. 2) demonstrated that DMIPP uptake and MBF positively correlated in normal myocardium (n = 897 samples): DMIPP uptake = 0.77 + 0.23 · MBF; r = 0.41, s.e.e. = 0.12, $p < 0.0001$. This relationship was significantly different (F-test, $p < 0.0001$) from the correlation in hypoperfused myocardium (n = 221

TABLE 2
MBF and DMIPP Uptake in Native and ECB-perfused Myocardium of the Control and Intervention Group

	Control (n = 4)			Intervention (n = 10)		
	Native	p*	ECB	Native	p*	ECB
MBF (ml · g^{-1} · min^{-1})	1.10 ± 0.21	n.s.	1.13 ± 0.18	1.10 ± 0.18	0.0001	0.49 ± 0.20
DMIPP uptake (10^{-2} %ID/g)	1.87 ± 0.55	n.s.	1.75 ± 0.52	1.18 ± 0.42	0.0001	0.75 ± 0.26
Subendo-to-subepicardium ratio						
MBF	1.09 ± 0.12	n.s.	1.06 ± 0.19	1.07 ± 0.10	0.0001	0.69 ± 0.25
DMIPP	1.22 ± 0.14	n.s.	1.20 ± 0.14	1.09 ± 0.04	0.0001	0.77 ± 0.24
Heterogeneity (CV)						
MBF	0.23 ± 0.06	n.s.	0.22 ± 0.06	0.23 ± 0.05	0.0001	0.59 ± 0.22
DMIPP	0.13 ± 0.05	n.s.	0.12 ± 0.05	0.13 ± 0.05	0.0001	0.37 ± 0.23
p†	0.0001		0.0001	0.0001		0.01
Agreement	0.19 ± 0.04	n.s.	0.20 ± 0.04	0.23 ± 0.07	0.0001	0.46 ± 0.19

*p-value of native vs. ECB-perfused myocardium.
†p-value of MBF vs. DMIPP.
n.s. = not significant.

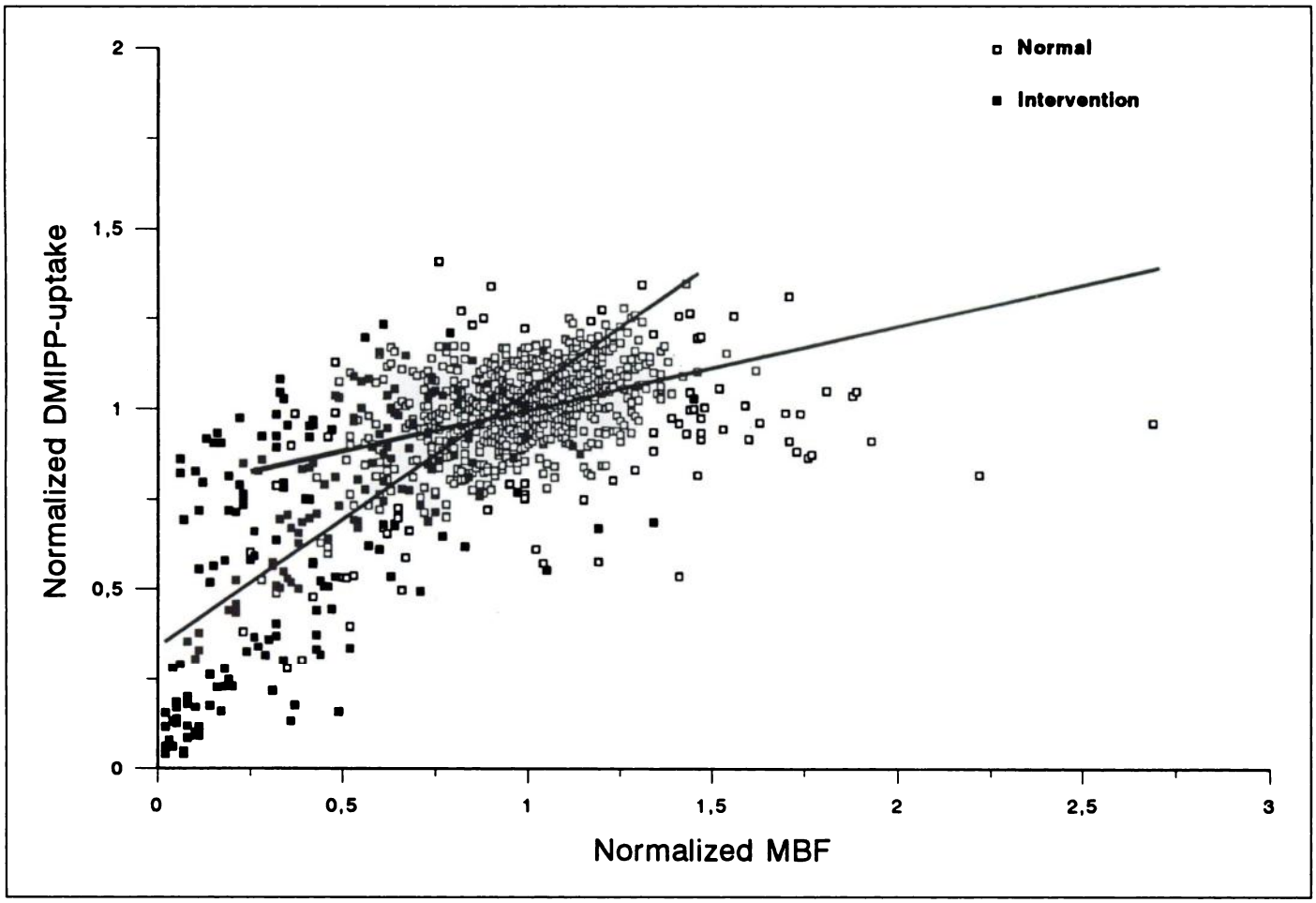

FIGURE 2. Relation between regional MBF and DMIPP uptake in the intervention group (10 dogs). All data are pooled and expressed relative to the mean of normal myocardium. DMIPP uptake and MBF correlated in normal myocardium (n = 897): DMIPP uptake = 0.77 + 0.23 · MBF; r = 0.41; s.e.e. = 0.12; $p < 0.0001$. This relationship was significantly different (F-test, $p < 0.0001$) from the correlation in hypoperfused myocardium (n = 221): DMIPP uptake = 0.35 + 0.70 · MBF; r = 0.63, s.e.e. = 0.25; $p < 0.0001$.

samples): DMIPP uptake = 0.35 + 0.70 · MBF; r = 0.63, s.e.e. = 0.25; $p < 0.0001$.

Heterogeneity of both MBF and DMIPP uptake increased significantly during hypoperfusion, whereas agreement between DMIPP uptake and MBF deteriorated significantly ($p < 0.0001$) from 0.23 ± 0.07 to 0.46 ± 0.19 (Table 2). For pooled data, heterogeneity in normal myocardium was 0.25 for MBF and 0.14 for DMIPP uptake, and in hypoperfused myocardium, these values were 0.66 and 0.45, respectively. Agreement, for pooled data, was 0.25 in normal compared to 0.78 in hypoperfused myocardium. These differences in heterogeneity between MBF and DMIPP uptake are illustrated by the distribution profiles in Figure 3.

Borderline Area

In six dogs, a borderline area was found that ranged from 6 to 18 samples, corresponding with 5.0% to 12.8% of the LV mass. In these six borderline areas, MBF was 0.94 ± 0.26 ml · g^{-1} · min^{-1} and DMIPP uptake 0.83 ± 0.10 × 10^{-2} %ID/g. Heterogeneity for MBF was 0.42 ± 0.08 and DMIPP uptake was 0.22 ± 0.10 ($p < 0.0001$).

DISCUSSION

DMIPP can detect hypoperfused myocardium because DMIPP uptake is reduced over a wide range of reduced MBF values. In flow-restricted areas, the overall DMIPP uptake was 66% ± 23% relative to normally perfused myocardium, whereas MBF was 45% ± 16%, indicating that reduction in DMIPP uptake was less pronounced than reduction of MBF. A possible explanation could be a compensatory increase in incorporation of fatty acids into triacylglycerols during ischemia (*29–31*) because DMIPP is preferentially incorporated into the neutral lipid pool (*8,12*). This phenomenon has also been suggested by Nishimura et al. (*32*), who studied BMIPP uptake in six dogs after a 3-hr occlusion of the LAD, followed by a 1-hr reperfusion. They found a mismatch of BMIPP/thallium uptake, with higher uptake of BMIPP.

In normal myocardium, there was a weak but significant correlation between MBF and DMIPP uptake. Moreover, linear regression analysis on a subset of samples with a relative regional myocardial flow greater than the normalized mean (469 samples) showed that DMIPP uptake did not correlate with flow at all. These findings indicate that flow is not the sole determinant of DMIPP uptake in normoxic myocardium. Although spatial differences in metabolic demand of normal myocardium have been suggested (*18,23–25*). Franzen et al. (*18*) showed an absence or only a weak correlation between regional MBF and metabolic parameters in normal canine myocardium. In contrast, a close correlation between BMIPP uptake, the monomethylated analog of DMIPP and intracellular ATP levels has been found (*33*). These observations suggest that regional DMIPP uptake could be more closely related to ATP content than to regional MBF. Further, in normal myocardium where a steady state prevails, we may assume that fatty acid uptake is closely related to fatty acid metabolism. There-

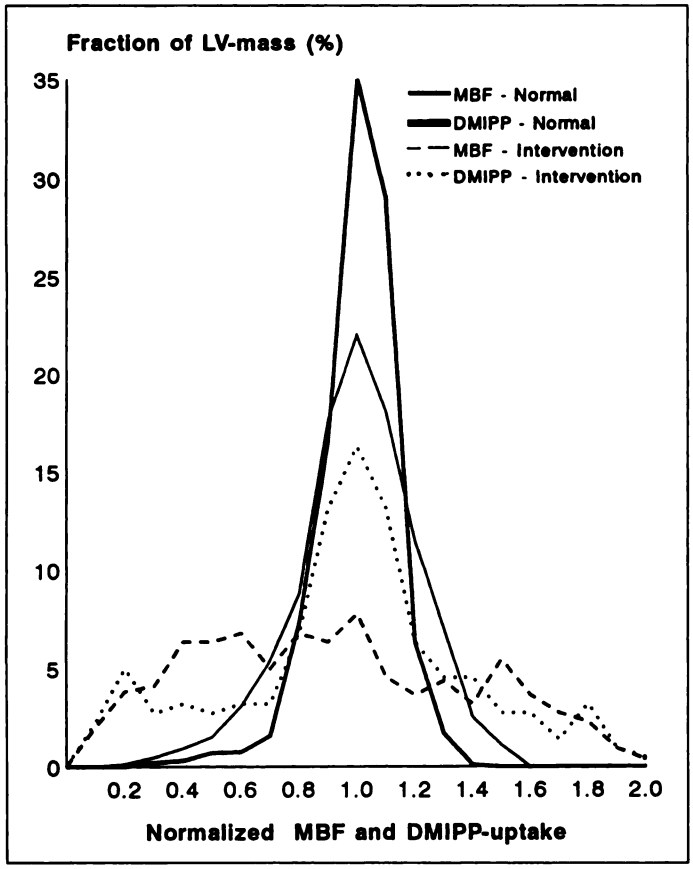

FIGURE 3. Frequency histogram (percentage of LV mass) of MBF and DMIPP uptake in normal (n = 897 samples) and hypoperfused (n = 221 samples) left ventricular myocardium of 10 dogs (pooled data of intervention group), normalized for the mean value of the normal and hypoperfused myocardial region of each dog.

fore, the more homogeneous distribution of DMIPP in normal myocardium than that in flow supports the hypothesis that heterogeneity in MBF is only partly explained by regional metabolic differences.

In hypoperfused myocardium, there was a significantly steeper slope of the relationship between DMIPP uptake and regional blood flow (DMIPP uptake = 0.70 · MBF + 0.35). Moreover, if only the samples with a regional MBF below 70% relative to the normal area (n = 181) were studied, we found an even steeper slope (DMIPP uptake = 1.06 · MBF + 0.25; r = 0.66, $p < 0.0001$). Thus, severity of reduction in MBF corresponds with DMIPP uptake. On the other hand, the level of reduction of DMIPP uptake on flow restriction varied considerably. The latter was shown by the disagreement between regional MBF and DMIPP uptake during flow reduction, as indicated by an increase of the heterogeneity of DMIPP uptake-to-MBF ratio: 0.23 ± 0.07 in normal compared to 0.46 ± 0.19 in hypoperfused myocardium. These differences in DMIPP uptake suggest regional differences in response to metabolic processes in cardiac tissue toward flow reduction.

Linear correlations between uptake of IFAs and MBF have been described over a wide range of flow values (*34–36*). Caldwell et al. (*35*) studied the relationship between radioiodinated paraphenylpentadecanoic acid and MBF in dogs during maximal exercise in combination with coronary occlusion and also found a significantly higher slope in the ischemic part compared to the normal part of the myocardium (0.39 compared to 0.25, respectively), but correlation coefficients were not different [0.68 and 0.74 (pooled data of absolute results), respectively]. However, the protocol they used created a wide range of MBF (0.05 ml · g^{-1} · min^{-1} to 7.58 ml · g^{-1} · min^{-1}), which largely contributed to the relatively high correlations compared to the present study. More recently, Reinhardt et al. (*36*) studied BMIPP uptake in rabbit hearts with an occlusion of the left circumflex artery and found linear correlations in both autoradiographic analysis (BMIPP uptake = 0.449 + 0.537 · MBF; r = 0.73) and segmental tissue analysis (BMIPP uptake = 0.058 + 0.881 · MBF; r = 0.94). These studies did not focus on heterogeneity of MBF or fatty acid uptake.

The heterogeneity we found for MBF in normal myocardium and the increase of heterogeneity during flow reduction are in line with previous studies (*16–25,27*). In normal myocardium, we found that DMIPP uptake was less heterogeneously distributed than MBF. Groeneveld et al. (*24*) recently also observed a lower heterogeneity for radioiodinated heptadecanoic acid than MBF (0.18 ± 0.05 compared to 0.23 ± 0.02, respectively). Heterogeneity of myocardial fatty acid uptake on this small tissue level during flow reduction has not been studied yet. Not only MBF but also DMIPP uptake became more heterogeneous in hypoperfused myocardium. The increase was relatively larger for DMIPP uptake, as it was for MBF; also, the agreement diminished. The increase of heterogeneity in MBF during flow reduction at the site of a major coronary artery has been demonstrated earlier, and this effect has been attributed to nonuniform loss of coronary flow reserve during underperfusion (*21,37*). It might be that nonuniform loss of coronary flow reserve during flow reduction results in regional differences of fatty acid uptake and even mismatching of flow and fatty acid uptake, as indicated by the increase of the disagreement between MBF and DMIPP uptake. Increased acidity, lactate and intracellular fatty acid levels affect the fatty acid uptake during flow reduction (*2*). Because local differences in these forementioned metabolic alterations in the flow deprived area can be anticipated, increased heterogeneity of fatty acid uptake might occur.

Uncoupling of myocardial fatty acid uptake and flow has been reported, albeit in different models of myocardial flow reduction; for instance, the 3-hr occlusion–reperfusion study by Nishimura et al. (*32*), mentioned above, showed relatively higher BMIPP uptake compared to flow in reperfused regions. We recently found that the majority of segments with a 18-fluorodeoxyglucose–perfusion mismatch in patients after subacute or old myocardial infarction, also showed a higher BMIPP uptake relative to perfusion (*38*). In contrast, a relatively lower BMIPP uptake compared to flow has been observed in patients after acute myocardial infarction or unstable angina. This issue has been reviewed in detail recently by Knapp et al. (*5,6*).

Methodological and Technical Considerations

In four control studies, we demonstrated that the ECB system, despite continuous instead of a more physiologic pulsatile flow, did not influence the pattern of DMIPP uptake or the heterogeneity in MBF compared to native perfused myocardium. Earlier, we have demonstrated that also metabolism of radioiodinated heptadecanoic acid in this particular model was not altered by the ECB system at normal flow rate (*39*). The use of heparin, required as anticoagulant for the ECB system, probably caused, by activation of lipoprotein kinase, a slight elevation of unlabeled plasma fatty acid level, as observed in this study.

By studying a moderate degree of flow reduction, we wanted to detect discrete changes in fatty acid uptake rather than gross changes that one could expect from a coronary occlusion model. A 30-min hypoperfused period was used because the major

alterations in fatty acid metabolism occur in the first 20–25 min (*2*). We waited another 40 min after DMIPP administration to assess its uptake because maximal DMIPP activity is reached at 20 min in normal myocardium, whereafter a plateau phase is found (*13*) and back-diffusion of small amounts of unmetabolized tracer is likely to occur until approximately 30 min after tracer administration (*40*).

The size of the samples are far below the limited resolution of devices used for in vivo imaging of patients. Nevertheless, a certain amount of tracer uptake in a particular segment of a planar or tomographic acquisition is a result of an apparently underlying heterogeneous tracer uptake. This heterogeneity is probably larger in perfusion defects or defects with reduced fatty acid uptake. This study may therefore lead to a better comprehension of the underlying pathophysiology in coronary artery disease patients with scintigraphic abnormalities.

The accuracy in the assessment of MBF and DMIPP uptake is discussed in the Appendix.

CONCLUSION

Because of its reduced uptake, radioiodinated DMIPP can identify regional hypoperfused myocardium. Yet, during hypoperfusion, heterogeneity of MBF and DMIPP uptake increases while agreement between MBF and DMIPP uptake deteriorates. The latter phenomenon demonstrates that there is serious uncoupling between fatty acid uptake and MBF during flow reduction. The more homogeneous distribution of DMIPP compared to flow in normal myocardium supports the hypothesis that heterogeneity in MBF is only partly explained by regional metabolic differences. These observations suggest that DMIPP uptake may provide additional, unique information on regional myocardial ischemia.

ACKNOWLEDGMENTS

Research at Oak Ridge National Laboratory was supported by the Office of Health and Environmental Research, United States Department of Energy, under Contract DE-AC05-960R22464 with Lockheed Martin Energy Systems Corporation. This study was supported in part by the Netherlands Heart Foundation Project 88.097. Animal preparations by B.J.H. van der Water, J. Grimbergen and G. Vink, and the opportunity to perform the experiments in the Radio Nuclide Centre of the Free University (Dr. J.P. van der Jagt Head) are greatly appreciated. We thank Viggo-Spectramed for the generous supply of medical equipment.

APPENDIX

Accuracy in the Assessment of MBF and DMIPP Uptake

Measurements of MBF in this study were performed with the microsphere technique (*28*). Buckberg et al. (*41*) demonstrated that at least 400 microspheres must be present in the tissue for accurate flow measurements. It can be deduced from our data that the samples from normal myocardium contained approximately 1000 microspheres. The relative method error (ME) can be assessed according to:

$$ME = \sqrt{\{1/b + (s.d./C)^2\}},$$

where b is the number of microspheres (i.e., approximately 1000), C is the number of radioactive counts in the tissue sample (which was always more than 10,000 in normal perfused samples) and s.d. is the standard deviation in the measurement of counts. Thus, the relative method error of our 1-g tissue samples was 3.3%. Previous studies (*16,19*) indicated an estimated error of 5.4% in 217-mg and 6%–7% in 170-mg samples. For DMIPP uptake, the relative method error is not known, but it will be small compared to the microsphere technique because the number of counts in the samples was always over 100,000 in normal samples.

Several studies dealing with regional differences in MBF have demonstrated that the observed heterogeneity is largely due to spatial heterogeneity rather than temporal heterogeneity (*10,37,38*). Because microspheres of 15 ± 1 μm are nearly fully trapped during a single passage through the capillary beds, temporal variability in the assessment of MBF using microspheres has to be considered. The observed variance, SD^2_{obs}, is the sum of the contributing variances:

$$SD^2_{obs} = SD^2_{spatial} + SD^2_{temporal} + SD^2_{method}.$$

King et al. (*16*) showed that the heterogeneity due to temporal heterogeneity was 0.09 in 170-mg samples. Assuming this value, although it is probably less because of a larger sample size, holds for the present study, it can be demonstrated from the above equation that the observed heterogeneity of 0.23 in normal myocardium will be close to the spatial heterogeneity of 0.21.

In contrast to the nearly 100% trapping of microspheres, the myocardial extraction of fatty acids under normal conditions is about 20%–40%. Comans et al. (*42*) showed that the extraction fraction of IHDA in man was 28% ± 6.4%, a value that correlated with the extraction of natural fatty acids. Based on a recent comparative study of IHDA, IPPA and DMIPP (*13*), we may assume that DMIPP extraction fraction will be lower than that of IHDA, leading to considerable amounts of circulating DMIPP during a 10-to-20-min period. Compared to assessment of MBF, temporal variability would be expected to contribute to a very low extent to the observed heterogeneity of DMIPP uptake. For these reasons, we may assume that for both MBF and DMIPP uptake, the observed heterogeneity will be largely determined by spatial heterogeneity.

REFERENCES

1. Opie LH. Metabolism of the heart in health and disease. Part I. *Am Heart J* 1968;76:685–698.
2. Van der Vusse GJ, Glatz JFC, Stam HCG, Reneman RS. Fatty acid homeostasis in the normoxic and ischemic heart. *Physiol Rev* 1992;72:881–940.
3. Visser FC, Sloof GW, Knapp FF. Myocardial metabolic imaging with iodine-123 fatty acids. In: Van der Wall EE, ed. *What's new in cardiac imaging*. Amsterdam: Kluwer Academic Publishers; 1992:229–247.
4. Visser PC, Bax JJ, Knapp FF Jr. Single photon imaging of myocardial metabolism: the role of ^{123}I-labeled fatty acids and ^{18}F deoxyglucose. In: Murray, Ell, eds. *Nuclear medicine in clinical diagnosis and treatment*. Churchill Livingstone; 1994:1239–1248.
5. Knapp FF Jr, Franken P, Kropp J. Cardiac SPECT with iodine-123-labeled fatty acids: evaluation of myocardial viability with BMIPP. *J Nucl Med* 1995;36:1022–1030.
6. Knapp FF Jr, Kropp J. Iodine-123-labeled fatty acids for myocardial single-photon emission tomography: current status and future perspectives. *Eur J Nucl Med* 1995;22:361–381.
7. Tamaki N, Kawamoto M, Yonekura Y, et al. Assessment of fatty acid metabolism using I-123 branched fatty acid: comparison with positron emission tomography. *Ann Nucl Med* 1993;7:SII-41–47.
8. Knapp FF Jr, Goodman MM, Callahan AP, Kirsch G. Radioiodinated 15-(p-iodophenyl)-3,3-dimethylpentadecanoic acid: a useful new agent to evaluate myocardial fatty acid uptake. *J Nucl Med* 1986;27:521–531.
9. Knapp FF Jr, Ambrose KR, Goodman MM. New radioiodinated methyl-branched fatty acids for cardiac studies. *Eur J Nucl Med* 1986;12:S39–S44.
10. Dudczak R, Schmoliner R, Angelberger P, Knapp FF, Goodman MM. Structurally modified fatty acids: clinical potential as tracers of metabolism. *Eur J Nucl Med* 1986;12:S45–S48.
11. Fink GD, Montgomery JA, David F, et al. Metabolism of beta-methyl-heptadecanoic acid in the perfused heart and liver. *J Nucl Med* 1990;31:1823–1830.
12. Yamamichi Y, Kusuoka H, Morishita K, et al. Metabolism of Iodine-123-BMIPP in perfused rat hearts. *J Nucl Med* 1995;36:1043–1050.
13. Sloof GW, Visser FC, Van Eenige MJ, et al. Comparison of uptake, oxidation and lipid distribution of 17-iodoheptadecanoic acid, 15-(p-iodophenyl)pentadecanoic acid and 15-(p-iodophenyl)-3,3-dimethylpentadecanoic acid in normal canine myocardium. *J Nucl Med* 1993;34:649–657.
14. Marcus ML, Kerber RE, Erhardt JC, Falsetti HL, Davis DM, Abboud FM. Spatial and temporal heterogeneity of left ventricular perfusion in awake dogs. *Am Heart J* 1977;94:748–754.
15. Sestier FJ, Mildenberger RR, Klassen GA. Role of autoregulation in spatial and temporal perfusion heterogeneity of canine myocardium. *Am J Physiol* 1978;235:H64–H71.
16. King RB, Bassingthwaighte JB, Hales JRS, Rowell LB. Stability of heterogeneity of myocardial blood flow in normal awake baboons. *Circ Res* 1985;57:285–295.

17. Bassingthwaighte JB, Malone MA, Moffet TC, King RB, Little SE, Link JM, Krohn KA. Validity of microsphere depositions for regional myocardial flows. *Am J Physiol* 1987;253:H184–H193.
18. Franzen D, Conway RS, Zhang H, Sonnenblick EH, Eng C. Spatial heterogeneity of local blood flow and metabolite content in dog hearts. *Am J Physiol* 1988;254:H344–H353.
19. Bassingthwaighte JB, King RB, Roger SA. Fractal nature of regional myocardial blood flow heterogeneity. *Circ Res* 1989;65:578–590.
20. Bassingthwaighte JB, Malone MA, Moffet TC, King RB, Chan IS, Link JM, Krohn KA. Molecular and particulate depositions for regional myocardial flows in sheep. *Circ Res* 1990;66:1328–1344.
21. Austiu RE Jr, Aldea GS, Coggins DL, Flynn AE, Hoffman JIE. Profound spatial heterogeneity of coronary reserve: discordance between patterns of resting and maximal myocardial blood flow. *Circ Res* 1990;67:319–331.
22. Groeneveld ABJ, Van Lambalgen AA, Van den Bos GC, Bronsveld W, Nauta JJP, Thys LG. Maldistribution of heterogeneous coronary blood flow during canine endotoxin shock. *Cardiovasc Res* 1991;25:80–88.
23. Groeneveld ABJ, Van Lambalgen AA, Van den Bos GC, Nauta JJP, Thijs LG. Metabolic vasodilatation with glucose-insulin-potassium does not change the heterogeneous distribution of coronary blood flow in the dog. *Cardiovasc Res* 1992;26:757–764.
24. Groeneveld ABJ, Visser FC. Correlation of heterogeneous blood flow and fatty acid uptake in the normal dog heart. *Basic Res Cardiol* 1993;88:223–232.
25. Bussemaker J, Van Beek HGM, Groeneveld ABJ, Hennekes M, Teerlink T, Thijs LG, Westerhof N. Local mitochondrial enzyme activity correlates with myocardial blood flow at basal work loads. *J Mol Cell Cardiol* 1994;26:1017–1028.
26. Van der Vusse GJ, Arts T, Glatz JFC, Reneman RS. Transmural differences in energy metabolism of the left ventricular myocardium: fact or fiction. *J Mol Cell Cardiol* 1990;22:23–37.
27. Flynn AE, Coggins DL, Austin RE Jr, et al. Nonuniform blood flow in the canine left ventricle. *J Surg Res* 1990;49:379–384.
28. Heyman MA, Payne BD, Hoffmann JIE, Rudolf AM. Blood flow measurements with radionuclide-labeled particles. *Prog Cardiovasc Dis* 1977;20:55–79.
29. Van der Vusse GJ, Roemen ThHM, Prinzen FW, Coumans WA, Reneman RS. Uptake and tissue content of fatty acids in dog myocardium under normoxic and ischemic conditions. *Circ Res* 1982;50:538–546.
30. Van der Vusse GJ, Stam H. Lipid and carbohydrate metabolism in the ischemic heart. *Basic Res Cardiol* 1987;82(suppl 1):149–153.
31. Van der Vusse GJ, Prinzen FW, Van Bilsen M, Engels W, Reneman RS. Accumulation of lipids and lipid-intermediates in the heart during ischemia. *Basic Res Cardiol* 1987;82(suppl. 1):157–167.
32. Nishimura T, Sagu M, Kihara K, et al. Fatty acid myocardial imaging using ^{123}I-beta-methyl-iodophenyl pentadecanoic acid (BMIPP): comparison of myocardial per fusion and fatty acid utilization in canine myocardial infarction (occlusion and reperfusion model). *Eur J Nucl Med* 1989;15:341–345.
33. Fujibayashi Y, Yonekura Y, Takemura Y, et al. Myocardial accumulation of iodinated beta-methyl-branched fatty acid analog, iodine-125-15-(p-iodophenyl)-3-(R,S)-methyl-pentadecanoic acid (BMIPP), in relation to ATP concentration. *J Nucl Med* 1990;31:1818–1822.
34. Reske SN, Schön S, Knust EJ, Machulla HJ, Eichelkraut W, Hahn N, Winkler C. Relation of myocardial blood flow and initial cardiac uptake of 15-(p-^{123}I-phenyl)pentadecanoic acid in the canine heart. *Nucl Med* 1984;23:83–85.
35. Caldwell JH, Martin GV, Link JM, Krohn KA, Bassingthwaighte JB. Indophenyl-pentadecanoic acid-myocardial blood flow relationship during maximal exercise with coronary occlusion. *J Nucl Med* 1990;30:99–105.
36. Reinhardt CP, Weinstein H, Marcel R, Leppo JA. Comparison of iodine-125-BMIPPA and thallium-201 in myocardial hypoperfusion. *J Nucl Med* 1995;36:1645–1653.
37. Coggins DL, Flynn AE, Austin RE Jr, Aldea GS, Muehrcke DD, Goto M, Hoffman JIE. Nonuniform loss of regional flow reserve during myocardial ischemia in dogs. *Circ Res* 1990;67:253–264.
38. Sloof GW, Visser FC, Bax JJ, Eersels J, Knapp FF, Teule GJJ. Comparison of BMIPP and FDG-uptake in ischemic heart disease. *J Nucl Med* 1996;37:184p.
39. Visser FC, Sloof GW, Comans E, Eenige van MJ, Knapp FF. Metabolism of radioiodinated 17-iodoheptadecanoic acid in the normal and ischemic dog heart [Abstract]. *Eur Heart J* 1990;11:137.
40. Fox KAA, Abendschein DR, Ambos HD, Sobel BE, Bergmann SR. Efflux of metabolized and nonmetabolized fatty acid from canine myocardium: implications for quantifying myocardial metabolism tomographically. *Circ Res* 1985;57:232–243.
41. Buckberg GD, Luck JC, Payne BE, Hoffman JIE, Archie JP, Fixler DE. Some sources of error in measuring regional blood flow with radioactive microspheres. *J Appl Physiol* 1971;31:598–604.
42. Comans EFI. Quantitation of myocardial fatty acid oxidation by scintigraphy with radioiodinated heptadecanoic acid. PhD thesis. Amsterdam: 1993.

Down-Regulation of Cardiac Muscarinic Receptors Induced by Di-Isopropylfluorophosphate

Héric Valette, André Syrota and Chantal Fuseau
Hospital Frédéric Joliot, Medical Research Department, French Atomic Agency, Orsay, France

The feasability of PET determination of myocardial muscarinic acetylcholine receptor (mAChR) density has been demonstrated in dogs and humans. The results of the PET method, however, were not validated by a direct comparison with the in vitro determination of mAChR density. **Methods:** Left ventricular mAChR concentrations were studied in beagle dogs at baseline and after a 5- or a 11-day treatment with the irreversible acetylcholinesterase inhibitor di-isopropylfluorophosphate (DFP). The determination of mAChR densities were performed in vivo using PET, ^{11}C-MQNB, the three-injection protocol and the compartmental model previously described. In a parallel group of dogs, determination of mAChR density was performed in vitro using ^{3}H-(-)-MQNB. **Results:** In control dogs (n = 4), PET left ventricular density of mAChR was 61.1 ± 8.1 pmol/ml tissue. In the 5-day DFP-treated animals (n = 3), Bmax decreased to 38.2 ± 8.3 pmol/ml tissue (−38%; p = 0.005 versus control). In the 11-day DFP-treated animals (n = 3), Bmax was 34.7 ± 5.5 pmol/ml tissue (−43%; p = 0.003). There was no change in the affinity constant either at 5 or 11 days. In control dogs, Bmax, measured in vitro, was 9.53 ± 0.93 pmol/g tissue. In the 5-day DFP-treated animals, Bmax decreased to 6.2 ± 0.9 pmol/g tissue (−35%; p = 0.003). In the 11-day DFP-treated animals, Bmax was 5.1 ± 0.6 pmol/g tissue (−47%; p = 0.003 versus control). At that time, there was no change in affinity constant. On the fifth and 11th days, myocardial acetylcholinesterase activity was reduced by 88% and 90%, respectively. **Conclusion:** The in vivo and in vitro methods showed a similar decrease in mAChR density while for both methods affinity constant remained unchanged. This study validates the ability of PET and of the compartmental model to in vivo quantify changes in mAChR density.

Key Words: muscarinic acetylcholine receptor; PET; methyl-quinuclidinyl-benzilate; di-isopropylfluorophosphate; down-regulation; heart

J Nucl Med 1997; 38:1430–1433

The neurotransmitter of the postganglionic parasympathetic system, acetylcholine, interacts with the heart through the action of the muscarinic acetylcholine receptors (mAChR). The in vivo myocardial characterization and quantification of these receptors were greatly facilitated by the development of ^{11}C-radiolabeled methyl-quinuclidinyl-benzylate (MQNB; *1–3*) and by that of compartmental analysis (*4–5*). The main goal of this study was to investigate the ability of PET and of compartmental analysis to assess changes in density of myocardial mAChR. Therefore, the changes in the PET values of mAChR density and of those of the in vitro measurements were compared. In experimental cardiac disease in large animals like dogs, changes

Received Jun. 20, 1996; revision accepted Nov. 27, 1996.
For correspondence or reprints contact: H. Valette, Service Hospitalier Frédéric Joliot, DRM-CEA, 4 Place du Général Leclerc, 91401 Orsay, France.